Doppler Estimation Based on Dual-HFM Signal and Speed Spectrum Scanning

Runyu Wei, Xiaochuan Ma, Shiduo Zhao, *Student Member, IEEE*, and Shefeng Yan, *Senior Member, IEEE*

***Abstract*—High-accuracy real-time Doppler estimation is one of the key problems in underwater acoustic communication systems. Using the dual-hyperbolic-frequency-modulation (dual-HFM) synchronous signal is an effective solution; however, the Doppler estimation accuracy is limited by the sampling frequency in the traditional methods. In this letter, we propose a high-accuracy speed spectrum scanning method based on the Doppler invariant and the frequency spectrum properties of the HFM signal. This signal processing system uses dual-HFM waveform as a synchronous signal, constructs the speed spectrum function at the receiver, and then obtains the Doppler estimate through one-dimensional scanning. This method breaks through the speed resolution limit induced by the sampling frequency in the traditional method and obtains a high-accuracy estimate. The influences of signal transmission and processing parameters on the Doppler estimation is analyzed, and the parameter selection criteria is presented to improve the reliability of the estimation. The results of both numerical simulation and underwater communication experiments prove the effectiveness of the proposed method.**

***Index Terms*—Doppler estimation, hyperbolic frequency modulation, underwater acoustic communication.**

I. Introduction

THE Doppler effect of underwater sound is much more severe than that of the radio for the propagation speed of sound waves is much slower than the speed of light. In areas such as underwater acoustic navigation, detection and confrontation, the Doppler estimation is an important part of the signal processor. In particular, in underwater acoustic communication and positioning systems, accurate real-time Doppler estimation is critical to the successful decoding of communication signals and the tracking of sound sources. Therefore, the issue of fast and high-accuracy Doppler estimation has received tremendous attention from researchers.

In underwater acoustic communication systems, Doppler estimation and compensation are required before demodulation [1]. The classical Doppler estimation method uses a set of correlators to calculate the correlation between different Doppler copies of the transmitted signal and the received signal, and the Doppler corresponding to the maximum correlation value is used as the estimate [1], [2]. While the resolution of this method increases as the number of correlators increases, the computational complexity increases significantly as well. Subsequently, researchers proposed a block Doppler estimation method [3]. In this scheme, two LFM signals are inserted before and after the data frame, and the two peaks outputted by the matched filters provide the estimate of the change in frame length, thereby obtaining the Doppler estimate. This method has been widely used and has been extended to variations such as the delayed cross-correlation method [4], [5]. However, this scheme loses real-time performance, and the estimation accuracy decreases significantly when the Doppler shift changes drastically during the processing period. The hyperbolic frequency modulation (HFM) signal is a Doppler-tolerant waveform that has been widely used by sonar systems [6]–[8]. In recent years, a Doppler estimation method based on two HFM signals with different frequency sweeping directions has gradually attracted attention [9]–[11]—this dual-HFM waveform is also called the Up-Mute-Down-HFM (UMD-HFM) signal [11]. While this method can realize fast real-time Doppler estimation, its performance is not robust in underwater acoustic channels. To fix this problem, a dual-HFM signal-based method using correlation peak matching (CPM) is proposed [12], which improves the robustness of traditional methods and has been experimentally verified. However, this method is designed based on time-domain correlators; thus, the Doppler resolution is limited by the sampling rate.

In view of the resolution limitation in the existing methods, a high-accuracy scheme for Doppler estimation based on the speed spectrum scanning is proposed in this letter. This method takes advantage of the Doppler invariance of the HFM signal and the frequency-domain properties of the differential HFM signal, allowing the radial speed estimate to be obtained through a one-dimensional search. Theoretical analysis shows that this method can achieve high-precision Doppler estimation under properly selected transmitting and processing parameters. Underwater communication experiments verify the effectiveness and the performance advantages of this method over the traditional dual-HFM signal-based methods.

The letter is organized as follows. Section II briefly introduces the theoretical basis of HFM signals. Section III derives and presents the proposed Doppler estimation method. Section IV shows the numerical simulation and underwater acoustic communication experiment results. Section V concludes with a brief summary.

II. Properties of HFM Signal

The HFM signal waveform with start frequency f_l, end frequency f_h and pulse duration T is expressed as

$$s\left(f_l, f_h, T, t\right) = \mathrm{Rect}\left(\frac{t}{T}\right) \cdot \exp\left[-j2\pi\frac{f_0^2}{M}\ln\left(1-\frac{M}{f_0}t\right)\right] \tag{1}$$

Manuscript received June 11, 2020; revised August 2, 2020; accepted August 18, 2020. Date of publication August 28, 2020; date of current version October 12, 2020. This work was supported by the National Natural Science Foundation of China under Grant 61725106, and by the Youth Innovation Promotion Association, Chinese Academy of Sciences. The associate editor coordinating the review of this manuscript and approving it for publication was Prof. Jun Liu. *(Corresponding author: Xiaochuan Ma.)*

The authors are with the Key Laboratory of Information Technology for Autonomous Underwater Vehicles, the Institute of Acoustics, Chinese Academy of Sciences (IACAS), Beijing 100190, China, and also with the University of Chinese Academy of Sciences, Beijing 100864, China (e-mail: weirunyu@mail.ioa.ac.cn; maxc@mail.ioa.ac.cn; zhaoshiduo16@mails.ucas.edu.cn; sfyan@ieee.org).

Digital Object Identifier 10.1109/LSP.2020.3020222

where $j = \sqrt{-1}$. $f_0 = \frac{2 f_l f_h}{f_l + f_h}$ is the instantaneous frequency of the HFM signal at $t = 0$, and $M = \frac{4 f_l f_h (f_h - f_l)}{(f_l + f_h)^2 \cdot T}$ is the frequency modulating factor. Under the premise that it will not cause confusion, f_l and f_h will be omitted, as they are always constant parameters in this letter. The instantaneous frequency of the HFM signal is

$$f_t(T, t) = \frac{f_0}{1 - \frac{M}{f_0} t}, \tag{2}$$

which is a hyperbolic function.

The Doppler estimation method proposed in this letter depends on two properties: the Doppler invariant property of the HFM signal and the spectral property of the differential HFM signal. The following is a brief introduction of these properties.

The HFM signal has similar properties to the LFM signal in narrow-band situation, but in wideband situation, the hyperbolic sweeping frequency makes the HFM signal "Doppler invariant" [13], [14]. When there is relative movement between the source and the receiver, the pulse width of the transmitted HFM signal is expanded, and the received waveform is

$$s(kt) = \mathrm{Rect}\left(\frac{kt}{T}\right) \exp\left[-j2\pi \frac{f_0^2}{M} \ln\left(1 - \frac{M}{f_0} \cdot kt\right)\right] \tag{3}$$

where $k = \frac{c}{c+v}$ is the scaling factor, v is the radial speed of the source away from the receiver, and c is the speed of sound. In active detection application scenarios, the scaling factor will be $k = \frac{c-v}{c+v}$. When $|v|/c$ is small, the difference between $\mathrm{Rect}(\frac{t}{T})$ and $\mathrm{Rect}(\frac{kt}{T})$ can be ignored, and

$$s(kt) = s\left(t - \varepsilon(k)\right) \cdot \exp\left(j\vartheta(k)\right) \tag{4}$$

is approximately satisfied on the definition domain, where $\varepsilon(k) = \frac{f_0}{M}(\frac{1}{k} - 1)$ and $\vartheta(k) = -2\pi \frac{f_0^2}{M} \ln k$. Therefore, the expanded signal is almost a time-shift of the original HFM signal. After the expansion, the instantaneous frequency of the waveform is still a hyperbola with modulating factor M, despite the slight change in the sweeping frequency range. The difference between $\mathrm{Rect}(\frac{t}{T})$ and $\mathrm{Rect}(\frac{kt}{T})$ is influential only if the bandwidth is fairly small or if the radial speed is significantly large. An extended HFM matched filter was proposed to deal with this bias [15].

The frequency spectrum of the HFM signal can only be accurately expressed by the incomplete gamma function [16]. However, the approximation within the frequency range (f_l, f_h) can be easily expressed. The use of (4) leads to an approximated spectrum within (f_l, f_h)

$$S(T, f) = C(T) \cdot \frac{1}{f} \cdot \exp\left[j2\pi \frac{f_0}{M}\left(f_0 \ln f - f + \varphi(T)\right)\right] \tag{5}$$

where $C(T)$ and $\varphi(T)$ are independent of f. For convenience, we will not expand these two factors. According to the Parseval's theorem, we have $\sqrt{\beta} C(T) = C(\beta T)$, where β is a positive real number. Making use of the derivative property of the Fourier transform, we obtain

$$\begin{aligned} &-\frac{j}{2\pi\sqrt{\beta}} \exp\left(j \cdot \theta\left(T, \beta\right)\right) \cdot \left(C(T)\right)^{\beta - 1} \cdot \frac{\mathrm{d}}{\mathrm{d}t} s\left(\beta T, t\right) \\ &= \mathcal{F}^{-1}\left[\left(f \cdot S(T, f)\right)^{\beta}\right] \end{aligned} \tag{6}$$

where

$$\theta\left(T, \beta\right) = 2\pi \frac{\beta f_0}{M}\left(\varphi(T) - \varphi\left(\beta T\right)\right) \tag{7}$$

is a factor independent of t. The differential HFM signal

$$\frac{\mathrm{d}}{\mathrm{d}t} s(T, t) = j2\pi f_t(T, t) \cdot s(T, t) \tag{8}$$

appearing on the left side of (6) is still a frequency modulation signal defined on $(-T/2, T/2)$, but its envelope $f_t(T, t)$ changes slowly (refer to (2)).

III. Doppler Estimation Based on Dual-HFM Signals

Let the transmit signal be the UMD-HFM signal defined in [11]

$$s_t(t) = s\left(f_h, f_l, T, t\right) + s\left(f_l, f_h, T, t - T - T_e\right) \tag{9}$$

as demonstrated in Fig. 1. The first term is a down-sweeping HFM signal and the second term is an up-sweeping HFM signal, and the whole signal is referred to as the "dual-HFM" signal in the following text. In this section, the superscript "(d)" represents the down-sweeping HFM signal, and the superscript "(u)" represents the up-sweeping HFM signal. Consider the case where the sound source is moving and the receiver is fixed. The received signal with Doppler effect can be expressed as

$$x(t) = A \cdot s_t\left(k\left(t - \tau\right)\right) \tag{10}$$

where A is the amplitude attenuation factor, $k = \frac{c}{c+v}$ is the waveform scaling factor, and τ is the propagation time (of the channel at $t = 0$). From (4), the received signal can be expressed as the time-shifted form of the HFM source signal in equation (11) shown at the bottom of this page, where M is set as the positive (i.e. absolute) value. Let the frequency spectrum of the down-sweeping HFM signal be defined as

$$S(f) = \mathcal{F}\left[s^{(d)}(T, t)\right] \tag{12}$$

The parameters of the transmit down-sweeping HFM signal are the default parameters when f_l, f_h and T are omitted in the followings. Since $\mathcal{F}[s^{(u)}(T, t)] = S^*(f)$, the absolute square spectrum of $x(t)$ can be written as equation (13) shown at the bottom of this page, where $\mathrm{Re}[\cdot]$ denotes the real part of the complex function, $\tau_1 = -\varepsilon(k)$, and $\tau_2 = \frac{1}{k}(T + T_e) + \varepsilon(k)$. To eliminate the influence of $S(f)$ and extract information about k, we define a statistic

$$U(f) = f^4 |X(f)|^2 \left(S(f)\right)^2 \tag{14}$$

$$x(t) = A \cdot \left[s^{(d)}\left(T, t - \left(\tau - \varepsilon(k)\right)\right) \cdot \exp\left(-j\vartheta(k)\right) + s^{(u)}\left(T, t - \left(\tau + \frac{1}{k}\left(T + T_e\right) + \varepsilon(k)\right)\right) \cdot \exp\left(j\vartheta(k)\right)\right] \tag{11}$$

$$|X(f)|^2 = 2A^2 \left\{|S(f)|^2 + \mathrm{Re}\left[\left(S(f)\right)^2 \cdot \exp\left(j2\pi f\left(\tau_2 - \tau_1\right)\right) \cdot \exp\left(-j2\vartheta(k)\right)\right]\right\} \tag{13}$$

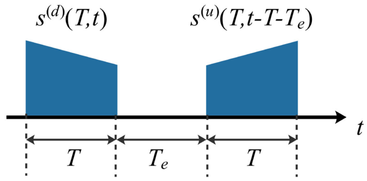

Fig. 1. Transmit signal structure.

within the frequency range (f_l, f_h). From (5) we have $f^4 = C^4|S(f)|^{-4} = f^2C^2|S(f)|^{-2}$, where $C = C(T)$. Substituting it into (13) and (14) gives (15) shown at the bottom of this page, where, the last term includes the complex exponential component with period $\Delta\tau = \tau_2 - \tau_1$. Hence, the estimate of $\Delta\tau$ can be obtained from the inverse Fourier transform of $U(f)$. Making use of (6) we have (16) shown at the bottom of this page, where $\theta(2)$ and $\theta(4)$ are constants, and $\delta(t)$ is the impulse function. The first differential HFM signal is defined in $(-T, T)$, while the second one is defined in $(-2T - \Delta\tau, 2T - \Delta\tau)$. Let T_{seg} be the processing interval length when the time-domain signal is transformed into frequency domain. To ensure that neither the period $(-T, T)$ nor $(-2T - \Delta\tau, 2T - \Delta\tau)$ covers $t = \Delta\tau$, it should be satisfied that

$$T < \Delta\tau \text{ and } T_{seg} - 2T - \Delta\tau > \Delta\tau \tag{17}$$

Considering that $\Delta\tau \approx T + T_e$ when $|v| \ll c$, then (17) reduces to

$$T_e > 0 \tag{18}$$

$$T_{seg} > 4T + 2T_e = 2(2T + T_e) \tag{19}$$

and the two inequalities should keep a certain margin. The inequality (18) suggests that there should be a gap between the down-sweeping and the up-sweeping HFM signals in the transmit waveform. The inequality (19) suggests that the signal should be extended to at least twice as long as the transmit waveform by padding zero before being transformed into the frequency domain. When these two inequalities are both satisfied, the impact of the first two terms in (16) in regards to the estimation of $\Delta\tau$ will be mostly eliminated.

However, because the time resolution of the IFFT output cannot be higher than the sampling interval, the accuracy of the estimated value of $\Delta\tau$ may not be ideal. Since the speed is $v = \frac{c\cdot[\Delta\tau - (T+T_e)]}{T+T_e+2f_0/M}$, the estimation error of the speed is

$$e(v) = \frac{c}{T + T_e + 2f_0/M} \cdot e(\Delta\tau) \tag{20}$$

Thus, the resolution unit of the speed estimate derived from the IFFT method is $\epsilon_v = \frac{c}{T+T_e+2f_0/M} \cdot \frac{1}{f_s}$, where f_s is the sampling frequency. Therefore, the resolution of the speed estimate is limited by the sampling frequency.

Using high-resolution line spectral estimation methods can obtain speed estimations with resolution higher than ϵ_v. Since there is only one periodic component in (15), the best estimate of periodic information can be simply obtained by scanning the "speed spectrum" with radial speed as the independent variable. In other words, assume that the possible range of the speed is (v_1, v_2), and then scan the spectrum with all the possible speeds within the range. Define the speed spectrum function as

$$Y(v) = \int_f U(f)\exp\left(j2\pi f\left(c_1 v + c_2\right)\right) \mathrm{d}f \tag{21}$$

where $c_1 = \frac{(T+T_e)+2f_0/M}{c}$ and $c_2 = T + T_e$ are both constants. The estimate of the radial speed is

$$\hat{v} = \underset{v\in(v_1,v_2)}{\arg\max} |Y(v)| \tag{22}$$

In fact, the speed spectrum scanning is the IDFT of (14) within a small range, which breaks the resolution limitation of IFFT on (14). A practicable procedure is to use IFFT for a rough search first, and then use spectrum scanning for high-precision search. It should be noted that the frequency-domain processing above is calculated within the frequency range (f_l, f_h) (or a little bit expanded according to [15]), and the components outside the range should set zero. This is because the frequency spectrum expression of the HFM signal given in Section II is only appropriate within the range (f_l, f_h). Moreover, since the received signal out of this range is mostly noise, the last term of (15) can hardly be a sinusoidal function outside the frequency range.

The steps in the proposed speed spectrum scanning algorithm can be summarized as follows:

1) Find the approximate location of the dual-HFM waveform in the received signal using matched filtering, and intercept a segment of signal containing the dual-HFM signal. Extend the intercepted signal segment to length T_{seg} by padding zero where $T_{seg} > 2(2T + T_e)$, and reserve a certain margin.
2) Calculate the frequency spectrum $X(f)$ of the zero-padded signal, and calculate the statistic $U(f)$ given by expression (14), where $X(f)$ is determined by (12). Note that the down-sweeping HFM signal should be extended to the same length as $X(f)$ by padding zero. If the bandwidth is not large enough or the Doppler shift is significant, the bandwidth can be appropriately increased [15] when calculating (12).
3) Scan the radial speed within the possible range of speed and calculate the speed spectrum $Y(v)$ defined by (21). The radial speed estimate $\hat{v}$ is given by (22).

IV. Simulation and Experimental Results

In this section, we present numerical simulation and underwater experimental results of the proposed Doppler estimation method. The underwater experiment is designed to test the reliability of the underwater communication system and the positioning performance of the multi-buoy network for underwater moving sources. The methods to be compared are matched-filter-based traditional method and CPM method, and [9], [12] provide a detailed introduction about them.

$$U(f) = A^2\left\{\begin{array}{c} 2C^2(f\cdot S(f))^2 + (f\cdot S(f))^4 \cdot \exp\left(j2\pi f\left(\tau_2 - \tau_1\right)\right)\cdot\exp\left(-j2\vartheta(k)\right) \\ +C^4\exp\left(-j2\pi f\left(\tau_2-\tau_1\right)\right)\cdot\exp\left(j2\vartheta(k)\right)\end{array}\right\} \tag{15}$$

$$\mathcal{F}^{-1}\left[U(f)\right] = A^2C^3\left\{-\frac{j}{4\pi}\left[\begin{array}{l} 2\sqrt{2}\exp\left(j\cdot\theta(2)\right)\cdot\frac{\mathrm{d}}{\mathrm{d}t}s^{(d)}\left(2T,t\right) \\ +\exp\left(j\cdot\theta(4)\right)\cdot\frac{\mathrm{d}}{\mathrm{d}t}s^{(d)}\left(4T,t+\Delta\tau\right)\end{array}\right] + C\delta\left(t-\Delta\tau\right)\cdot\exp\left(j2\vartheta(k)\right)\right\} \tag{16}$$

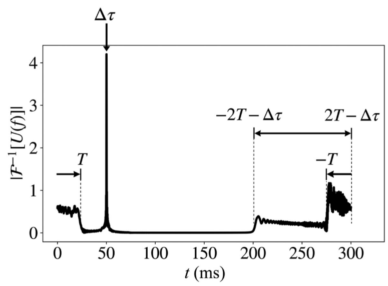

Fig. 2. IFFT result of $U(f)$ (without noise).

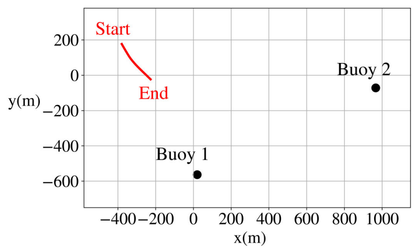

Fig. 3. Underwater communication experiment configuration.

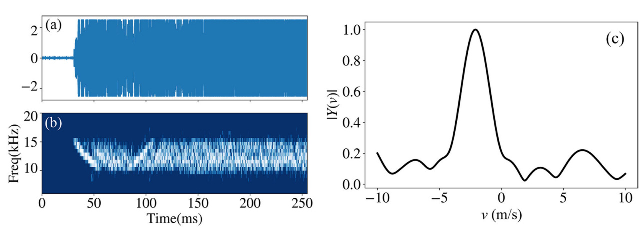

Fig. 4. (a, b) Received waveform and spectrogram; (c) The speed spectrum $|Y(v)|$ of underwater moving source (actual speed: $v_{real} = -2.13$ m/s).

Firstly, the properties of $\mathcal{F}^{-1}[U(f)]$ without noise are demonstrated by numerical simulation. The parameters used in the computer simulation are as follows: dual-HFM signal parameters $f_l = 4$ kHz, $f_h = 8$ kHz, $T = T_e = 25$ ms, $f_s = 50$ kHz; speed parameters $v = 2$ m/s, $c = 1500$ m/s; signal processing parameter $T_{seg} = 300$ ms. After calculating $U(f)$ with (14) and performing IFFT, the output time-domain signal is shown in Fig. 2. It can be seen that the peak of $|\mathcal{F}^{-1}[U(f)]|$ is approximately at $\Delta\tau \approx T + T_e$, and two differential HFM signals are located at $(-T, T)$ and $(-2T - \Delta\tau, 2T - \Delta\tau)$, respectively. The numerical simulation result under ideal noiseless conditions verifies the deduction in (16). Therefore, appropriate selection of signal transmission and processing parameters can effectively avoid the influence of the two differential HFM signals on the detection of the periodic component in $U(f)$.

Next, a set of experimental sonar data is used to test the proposed Doppler estimation method. The field trial data was collected in Thousand Island Lake, China, in March 2018. As shown in Fig. 3, the transducer mounted 3 m-deep moved along the trajectory at an average speed 2.15 m/s, and two hydrophones (approximately 1.5 m deep) were attached to buoys. The actual position of the transducer and the buoys are provided by GPS. The source transmitted communication data frames every 2 seconds with dual-HFM signal as the preamble. The transmission parameters are: $f_l = 10$ kHz, $f_h = 15$ kHz, $T = T_e = 25.6$ ms, and $f_s = 80$ kHz.

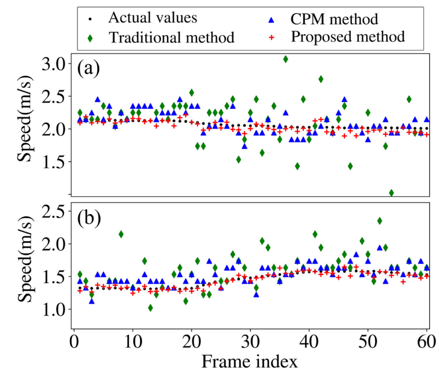

Fig. 5. Estimation results of target radial speed (60 frames).

TABLE I
RMSE OF THE RADIAL SPEED ESTIMATES (M/S)

	Buoy 1	**Buoy 2**
Traditional method	1.394	1.417
CPM method	0.159	0.147
Proposed method	0.060	0.046

Taking a received frame of buoy 1 as an example, Fig. 4(a) shows the waveform after bandpass filtering, and Fig. 4(b) shows the time-frequency spectrogram. The dual-HFM signal can be observed in the spectrogram. We process the intercepted signal using the proposed method, where $T_{seg} = 300$ ms and the speed scanning range is $(-10$ m/s, 10 m/s$)$. The result of $|Y(v)|$ is given in Fig. 4(c). The spectrum peak gives the radial speed estimate $\hat{v} = -2.092$ m/s, while the actual value from GPS data is $v_{real} = -2.13$ m/s.

Using the method proposed above, we process the continuous 60 frames of data from the two buoys. The radial speed estimation results are plotted in Fig. 5, where the speed of the source moving closer to the receiver is defined as positive. The traditional method and the CPM method are employed for comparison. The root mean square error (RMSE) of the estimates are given in Table I, and Fig. 5 and Table I show that the proposed method shows a further improvement in estimation performance than the methods introduced in [12]. The performance improvement comes from two aspects: on the one hand, the appropriate transmission and processing parameters reduce the interference in the peak detection; on the other hand, the speed spectrum scanning breaks through the resolution limit ϵ_v, and achieves the continuous estimation of the target speed.

V. CONCLUSION

In this letter, we introduce a novel Doppler estimation method based on the dual-HFM signal and speed spectrum scanning. Through theoretical analysis, appropriate transmission and processing parameters are selected, reducing the interference in speed spectrum peak detection and thereby increasing the accuracy of the estimation. In addition, the speed spectrum scanning breaks through the speed resolution limit by the sampling frequency and realizes the continuous estimation. The numerical simulation and the underwater communication experiment verify the effectiveness of the method, as well as the application prospect of the dual-HFM signal in the field of underwater communication synchronization and underwater target detection and tracking.

REFERENCES

[1] M. Stojanovic, J. A. Catipovic, and J. G. Proakis, "Phase-coherent digital communications for underwater acoustic channels," *IEEE J. Ocean. Eng.*, vol. 19, no. 1, pp. 100–111, Jan. 1994.

[2] M. Johnson, L. Freitag, and M. Stojanovic, "Improved Doppler tracking and correction for underwater acoustic communications," in *Proc. Int. Conf. Acoust., Speech, Signal Process.*, 1997, vol. 1, pp. 575–578.

[3] B. S. Sharif, J. Neasham, O. R. Hinton, and A. E. Adams, "A computationally efficient Doppler compensation system for underwater acoustic communications," *IEEE J. Ocean. Eng.*, vol. 25, no. 1, pp. 52–61, Jan. 2000.

[4] C. He, J. Huang, Q. Meng, and Q. Zhang, "Accurate Doppler factor estimation for multipath underwater acoustic channels," *Audio Eng.*, vol. 34, no. 12, pp. 57–59, 2010.

[5] J. Trubuil and T. Chonavel, "Accurate Doppler estimation for underwater acoustic communications," in *Proc. Oceans Conf.*, Yeosu, South Korea, 2012, pp. 1–5.

[6] L. Zhang, X. Xu, W. Feng, and Y. Chen, "HFM spread spectrum modulation scheme in shallow water acoustic channels," in *Proc. Oceans Conf.*, Hampton Roads, VA, USA, 2012, pp. 1–6.

[7] J. Marszal and R. Salamon, "Distance measurement errors in silent FM-CW sonar with matched filtering," *Metrology Meas. Syst.*, vol. 19, no. 2, pp. 321–332, 2012.

[8] M. Wang, Z. Li, S. Wu, J. Qin, and Y. Yu, "The characteristic of sound propagation in deep water and underwater source localization in the direct zone," *Chinese J. Acoust.*, vol. 38, no. 4, pp. 433–444, 2019.

[9] X. Zhang, F. Kong, and H. Feng, "Frequency offset estimation and synchronization of underwater acoustic communication with hyperbolic frequency modulation signal," *Tech. Acoust.*, vol. 29, no. 2, pp. 210–213, 2010.

[10] K. Wang, S. Chen, C. Liu, Y. Liu, and Y. Xu, "Doppler estimation and timing synchronization of underwater acoustic communication based on hyperbolic frequency modulation signal," in *Proc. Int. Conf. Netw., Sens. Control*, 2015, pp. 75–80.

[11] M. Xin, W. Li, X. Wang, Y. Zhang, and L. Xu, "Preamble design with HFMs for underwater acoustic communications," in *Proc. Oceans Conf.*, Kobe, Japan, 2018, pp. 1–5.

[12] S. Zhao, S. Yan, and L. Xu, "Doppler estimation based on HFM signal for underwater acoustic time-varying multipath channel," in *Proc. Int. Conf. Signal Process., Commun. Comput.*, 2019, pp. 1–6.

[13] A. W. Rihaczek, "Doppler-tolerant signal waveforms," *Proc. IEEE*, vol. 54, no. 6, pp. 849–857, Jun. 1966.

[14] J. Yang and T. K. Sarkar, "Doppler-invariant property of hyperbolic frequency modulated waveforms," *Microw. Opt. Technol. Lett.*, vol. 48, no. 6, pp. 1174–1179, 2006.

[15] J. J. Murray, "On the Doppler bias of hyperbolic frequency modulation matched filter time of arrival estimates," *IEEE J. Ocean. Eng.*, vol. 44, no. 2, pp. 446–450, Apr. 2019.

[16] J. J. Kroszczynski, "Pulse compression by means of linear-period modulation," *Proc. IEEE*, vol. 57, no. 7, pp. 1260–1266, Jul. 1969.